

Finite Density Lattice Gauge Theories with Positive Fermion Determinants ^{*)}

D. K. Sinclair¹
J. B. Kogut² and D. Toublan²

¹*HEP Division, Argonne National Laboratory, 9700 South Cass Avenue, Argonne, IL 60439, USA*

²*Department of Physics, University of Illinois, 1110 West Green Street, Urbana, IL 61801, USA*

We perform simulations of (3-colour) QCD with 2 quark flavours at a finite chemical potential μ_I for isospin (I_3), and of 2-colour QCD at a finite chemical potential μ for quark number. At zero temperature, QCD at finite μ_I has a mean-field phase transition at $\mu_I = m_\pi$ to a superfluid state with a charged pion condensate which spontaneously breaks I_3 . We study the finite temperature transition as a function of μ_I . For $\mu_I < m_\pi$, where this is closely related to the transition at finite μ , this appears to be a crossover independent of quark mass, with no sign of the proposed critical endpoint. For $\mu_I > m_\pi$ this becomes a true phase transition where the pion condensate evaporates. For μ_I just above m_π the transition seems to be second order, while for larger μ_I it appears to become first order. At zero temperature, 2-colour QCD also possesses a superfluid state with a diquark condensate. We study its spectrum of Goldstone and pseudo-Goldstone bosons associated with chiral and quark-number symmetry breaking.

§1. Introduction

We are interested in QCD at finite baryon-number, isospin and strangeness densities at zero and at finite temperature. Finite baryon-number is of most interest, but most difficult to simulate. QCD at finite chemical potential μ for quark number has a complex fermion determinant which prevents the use of standard simulation methods.

We are studying theories which possess *some* of the properties of QCD at finite μ , but have positive fermion determinants. This allows us to use standard (hybrid molecular-dynamics) simulations.

2-colour QCD at finite μ has a positive fermion pfaffian and is amenable to simulations.^{1),2)} It has a sensible meson spectrum, but unphysical ‘baryon’ spectrum. At $\mu = m_\pi/2$, it undergoes a phase transition to a superfluid state with a diquark condensate and Goldstone bosons.^{3),4),5)} This is the analogue of the colour superconducting state suggested for QCD at finite μ . We have also studied this theory at non-zero temperature.⁶⁾ Here we summarize our calculation of the spectrum of (pseudo)-Goldstone bosons which characterize the pattern of symmetry breaking for this theory.⁷⁾

QCD at a finite chemical potential μ_I for isospin (I_3), has a positive fermion determinant which allows simulations.⁸⁾ It undergoes a phase transition at $\mu_I = m_\pi$

^{*)} Talk presented by D. K. Sinclair at *Finite Density QCD at Nara*, Nara, Japan, 10th-12th July, 2003.

to a superfluid state with a charged pion condensate which breaks I_3 and parity spontaneously, with associated charged Goldstone pions.^{9),10)}

Let us now compare the proposed phase diagrams for QCD at finite μ ^{11),12)} and QCD at finite μ_I (figure 1). Both show crossovers (dashed lines) at small chemical potential. For QCD at finite μ 1a the 2 solid lines which intersect the $T = 0$ axis and end in open circles (critical points) are expected to be first order. The order of the transition between the colour-superconducting and quark-gluon plasma phases is unknown. For QCD at finite μ_I , the solid lines to the left of the open circle (tricritical point) are second order, while that to the right is first order.

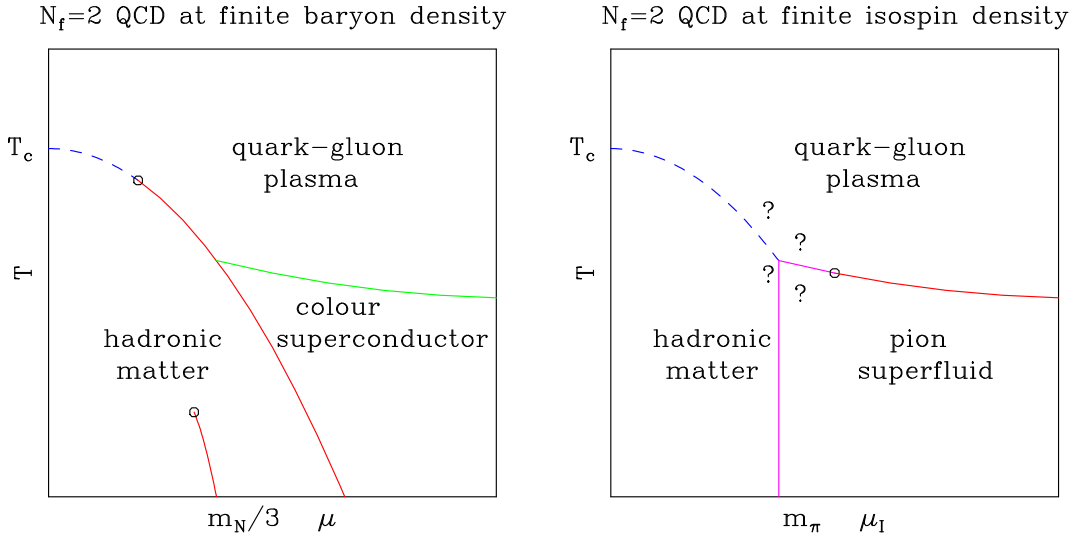


Fig. 1. a) Proposed phase diagram for QCD at finite quark-number chemical potential μ and temperature T . b) Proposed phase diagram for QCD at finite isospin chemical potential μ_I and temperature T .

We are studying 2-flavour QCD at finite μ_I and temperature in the neighbourhood of the finite temperature transition.^{14),15)} At low μ_I this transition from hadronic matter to a quark-gluon plasma is related to the corresponding transition at finite μ . Our predictions for the small μ behaviour of the finite temperature transition can be compared directly with those obtained by de Forcrand and Philipsen by continuing from imaginary μ .¹³⁾ These results will also be compared with results obtained using the series methods of the Bielefeld-Swansea collaboration.^{16),17)} They could also be checked using the reweighting methods of Fodor and Katz.^{18),19),20)} We are also simulating this theory at large μ_I where the finite temperature transition occurs at the point where the pion condensate evaporates. It is therefore a true phase transition. In particular we wish to determine where this transition changes from second order to first.⁸⁾

Section 2 gives our results for lattice QCD at finite μ_I and zero temperature. In Section 3 we present preliminary results for QCD at finite μ_I and temperature. The (pseudo)-Goldstone spectrum for 2-colour lattice QCD at finite μ is given in section 4. In section 5 we indicate how our new χ QCD action might help overcome

some of the problems at finite μ/μ_I . Section 6 gives our conclusions and suggests future directions for investigation.

§2. Lattice QCD at finite μ_I

The staggered quark action for lattice QCD at finite μ_I is

$$S_f = \sum_{\text{sites}} \left[\bar{\chi} \left[\mathcal{D} \left(\frac{1}{2} \tau_3 \mu_I \right) + m \right] \chi + i \lambda \epsilon \bar{\chi} \tau_2 \chi \right] \quad (2.1)$$

where $\mathcal{D}(\frac{1}{2}\tau_3\mu_I)$ is the standard staggered quark \mathcal{D} with the links in the $+t$ direction multiplied by $\exp(\frac{1}{2}\tau_3\mu_I)$ and those in the $-t$ direction multiplied by $\exp(-\frac{1}{2}\tau_3\mu_I)$. The λ term is an explicit I_3 symmetry breaking term required to see spontaneous symmetry breaking on a finite lattice. The determinant

$$\det[\mathcal{D}(\frac{1}{2}\tau_3\mu_I) + m + i\lambda\epsilon\tau_2] = \det[\mathcal{A}^\dagger \mathcal{A} + \lambda^2], \quad (2.2)$$

where

$$\mathcal{A} \equiv \mathcal{D}(\frac{1}{2}\mu_I) + m, \quad (2.3)$$

is positive allowing us to use standard hybrid molecular dynamics simulations.

This lattice action has a global $U(2) \times U(2)$ flavour symmetry when $m = \mu_I = \lambda = 0$. This breaks spontaneously to $U(2)$, with 4 Goldstone pions. When $\mu_I = 0$ but $m \neq 0$, this is reduced to $U(2)_V$, and the would-be-Goldstone pions gain a mass by PCAC. If $m = 0$, but $\mu_I \neq 0$, the symmetry is reduced to $U(1) \times U(1) \times U(1) \times U(1)$. Finally, if $m \neq 0$ and $\mu_I \neq 0$, the symmetry is further reduced to $U(1)_V \times U(1)_V$.

As μ_I is increased from zero, the effective mass of the π^+ is reduced to

$$m_\pi(\mu_I) = m_\pi - \mu_I, \quad (2.4)$$

which vanishes at $\mu_I = m_\pi$. For $\mu_I \geq m_\pi$, the $U(1)_V$ symmetry associated with τ_3 is broken spontaneously by a charged pion condensate

$$i \langle \bar{\chi} \epsilon \tau_2 \chi \rangle \Leftrightarrow i \langle \bar{\psi} \gamma_5 \tau_2 \psi \rangle. \quad (2.5)$$

The charged pion excitation created by

$$i \bar{\chi} \epsilon \tau_1 \chi \quad (2.6)$$

is the associated Goldstone boson. When λ is non-zero this gains a mass. Note that if $m = 0$, there will actually be 2 Goldstone bosons.

Simulations of lattice QCD at finite μ_I were performed with $m = 0.025$ and $\lambda = 0.0025, 0.005$ on an 8^4 lattice.⁸⁾ Figure 2 shows the diquark and chiral condensates as functions of μ_I . For m_π and μ_I small one can use chiral perturbation theory to predict the behaviour of this theory.^{9),10)} At tree-level this shows the phase transition at $\mu_I = m_\pi$. For $\mu_I > m_\pi$, the condensate rotates from the chiral direction towards the pion condensate direction so that I_3 breaks spontaneously. Indications are that at

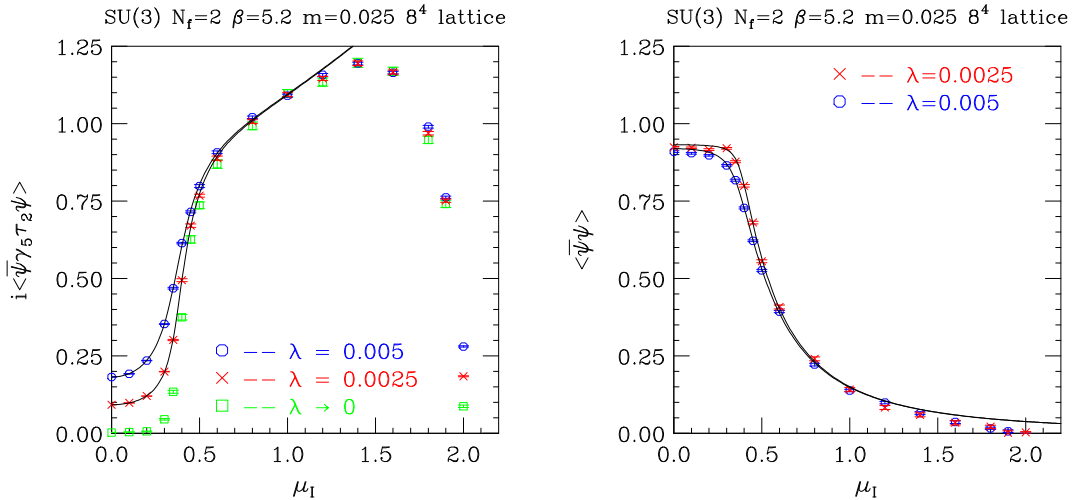


Fig. 2. a) Charged pion condensate as a function of I_3 chemical potential μ_I . The curves are a fit to mean-field scaling. b) Chiral condensate as a function of chemical potential μ_I . The curves are predictions from the fits to the pion condensate.

higher orders, the transition remains at $\mu_I = m_\pi$, but the rotation of the condensate is accompanied by an increase of its magnitude. However, the transition remains mean-field. We model this behaviour by fitting to a scaling form based on the tree-level predictions of a chiral Lagrangian of the linear sigma model form which allows the magnitude of the condensate to vary, while retaining the other predictions of chiral perturbation theory, with only one additional fitting parameter. The fits are shown on the figures. These indicate that there is a phase transition with mean-field exponents to a state where I_3 and parity are broken spontaneously. These fits also predict how the I_3 density increases from zero above m_π , and are in accord with the data (not shown) provided μ_I is not too large.

§3. Lattice QCD at finite μ_I and T

We first consider the finite temperature transition for $\mu_I < \mu_c$. As μ_I is increased from zero, the β_c of the crossover from hadronic matter to a quark gluon plasma decreases. Note, the results in this section should be considered preliminary.

We have performed simulations on an $8^3 \times 4$ lattice at $m = 0.05$ and $\lambda = 0$, at values of μ_I up to 0.55, which is very close to μ_c .^{14),15)} The position of the crossover is determined from the maxima of the susceptibilities for the plaquette, the chiral condensate, the Wilson line (Polyakov Loop) and the isospin density. As we shall see, there is consistency between these estimates. (The close proximity of the transitions in these various observables has been noted by many authors. Recently attempts to understand the reason for this have been made for zero μ/μ_I .²¹⁾ Combining this with earlier observations for finite μ ,²²⁾ it seems probable that this argument works at finite μ (and hence μ_I). A detailed analysis in terms of effective field theories, which also indicates applicability to finite μ/μ_I , has been given in^{23),24)}.) We use

Ferrenberg-Swendsen reweighting²⁵⁾ to determine these values with some precision. For the chiral condensate and isospin density which are determined from stochastic estimators, we use 5 noise vectors to calculate the susceptibilities, discarding the diagonal terms to obtain an unbiased estimate.

In figure 3 we show the Thermal Wilson Line (Polyakov Loop) as a function of $\beta = 6/g^2$ for a selection of μ_I values in this range. First it is clear that for each μ_I there is a rapid crossover from hadronic matter to a quark-gluon plasma over an interval $\Delta\beta \sim 0.05$. What we also notice is that the β of the crossover decreases monotonically with increasing μ_I .

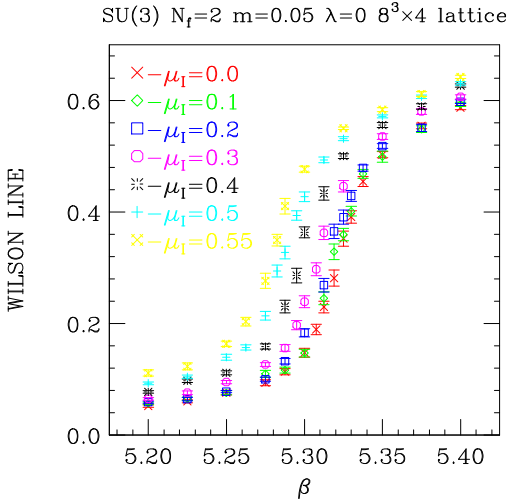


Fig. 3. Wilson Line as a function of $\beta = 6/g^2$ for μ_I values ≤ 0.55 .

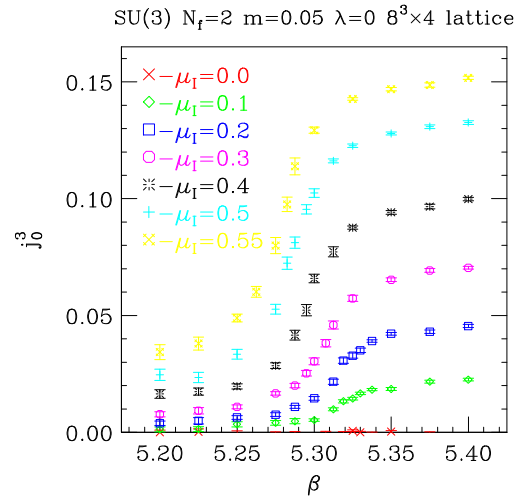


Fig. 4. Isospin density as a function of $\beta = 6/g^2$ for μ_I values ≤ 0.55 .

The corresponding graph for the I_3 density is given in figure 4. Here, not only does the β value for the cross over decrease with increasing μ_I , the value of this density increases with increasing μ_I . This is expected, since when μ_I is increased, it raises the level of the fermi sea, and hence the excess of $I_3 = 1/2$ quarks over $I_3 = -1/2$ quarks.

In figure 5 we show the Wilson Line susceptibility and in figure 6 we show the susceptibility for the isospin density. The chiral and plaquette susceptibilities are similar to that for the Wilson Line. The susceptibility for an operator \mathcal{O} is defined as

$$\chi_{\mathcal{O}} = V \langle \mathcal{O}^2 - \langle \mathcal{O} \rangle^2 \rangle, \quad (3.1)$$

where V is the space-time volume of the lattice. The peak of the susceptibility serves to define the position of the crossover. Clearly the measurements in these plots are inadequate to give precise positions of the peaks. However we can make a Ferrenberg-Swendsen reweighting of our ‘data’ at β values close to the peaks, which yields a more precise estimate of their positions.

We plot our estimates of β_c versus μ_I^2 from these 4 susceptibilities in figure 7, since we expect the leading dependence to be quadratic in μ_I . The straight line in

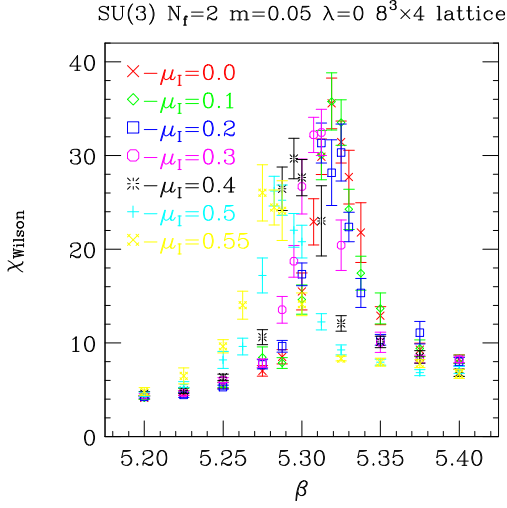


Fig. 5. Wilson Line susceptibility as a function of $\beta = 6/g^2$ for μ_I values ≤ 0.55 .

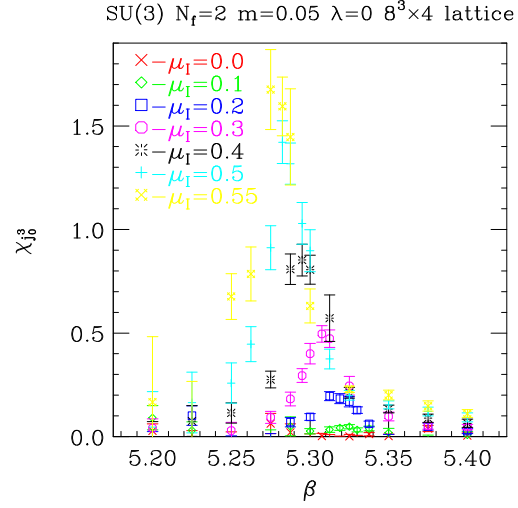


Fig. 6. Isospin susceptibility as a function of $\beta = 6/g^2$ for μ_I values ≤ 0.55 .

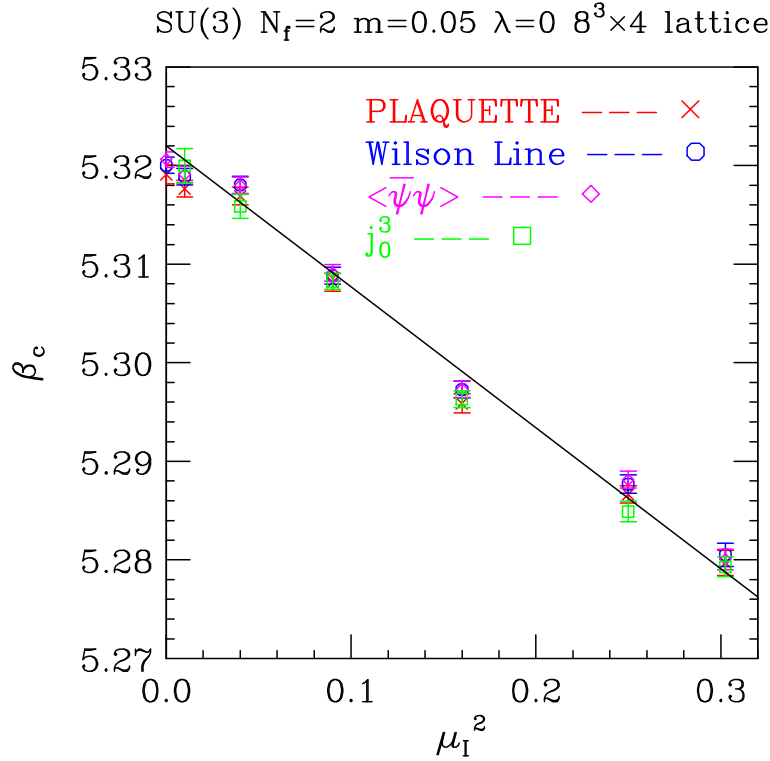


Fig. 7. β_c determined from the maxima of the susceptibilities, as a function of μ_I^2 .

this graph

$$\beta_c = 5.322 - 0.143\mu_I^2, \quad (3.2)$$

is not a proper fit and is only meant to be a rough guide. If we assume that at

$\mu_I = 0$, $T_c \approx 173$ MeV, then 2-loop running of the coupling would predict that for the highest μ_I considered, $T_c(\mu_I = 0.55) \approx 164$ MeV. Hence the relatively weak dependence of β_c on μ_I does translate into a relatively small change in T_c over a fairly large range of μ_I .

The Swansea-Bielefeld collaboration have determined that, for quark-number chemical potential μ small enough, the phase of the fermion determinant is well enough behaved that simulating with the magnitude of the determinant and including the phase factor in the measurements should work. This means that, to the extent that the position of the crossover is a well-defined quantity (i.e. is the same for all observables), the dependence of T_c on μ and μ_I should be identical for small μ , in particular,

$$\beta_c(\mu) = \beta_c(\mu_I = 2\mu) \quad (3.3)$$

so we can predict the small μ behaviour of β_c and hence T_c . Our results in equation 3.2, using equation 3.3, appear to be in agreement with those of de Forcrand and Philipsen¹³⁾

This also suggests that we should look for a critical point where the crossover becomes a first order transition, since such a critical endpoint is predicted for QCD at a finite chemical potential μ for quark number. For the $m = 0.05$ simulations reported here, we see no evidence for this for $\mu_I \leq 0.55$ (i.e. for $\mu_I < \mu_c$). However, $\mu_I = 0.55$ is equivalent to $\mu = 0.275 \approx 180$ MeV ($\mu_B = 535$ MeV), which is less than μ measured for the critical point by Fodor and Katz.^{18),19),20)} (Note, however, that the Fodor-Katz simulations are for 2+1-flavours, not 2.) We are therefore performing simulations with $m = 0.1$ and $m = 0.2$ where μ_c is beyond the Fodor-Katz value. However, we still see no signals (so far) for first-order behaviour. Thus we conclude that if there is a transition to be identified with this critical point, its μ_I increases with increasing mass, which is not unexpected.

Now let us turn to our studies of the finite temperature transition for larger μ_I s. For $\mu_I > \mu_c$, the pion condensate evaporates at the finite temperature transition. Thus here the finite temperature transition *is* a phase transition. At low temperatures, by approaching this phase boundary in the μ_I direction we have determined that the transition is second order. We now have preliminary evidence that for $m = 0.05$, $\lambda = 0.005$ and $N_t = 4$, the $\mu_I = 0.8$ transition is first order, based on simulations on $8^3 \times 4$ and $16^3 \times 4$ lattices, and are in the process of determining the position of the tricritical point.

We note that this transition is at $\beta_c \approx 5.2675$ i.e. at $T_c \approx 162$ MeV. This μ_I value is equivalent to $\mu = 0.4 \approx 259$ MeV. Hence the tricritical point must be close to the Fodor-Katz critical endpoint where $T_c \approx 160$ MeV, $\mu \approx 242$ MeV. We can therefore speculate that these 2 transitions are somehow related. Figure 8a shows the pion condensate as a function of β on a $16^3 \times 4$ lattice at $\mu = 0.8$. Figure 8b shows the time evolution of this condensate from hot and cold starts at $\beta = 5.2675$, showing evidence for coexisting states. Our “time” increment for updating $dt = 0.02$ was larger than desirable so we are repeating our simulations with $dt = 0.01$ close to the transition.

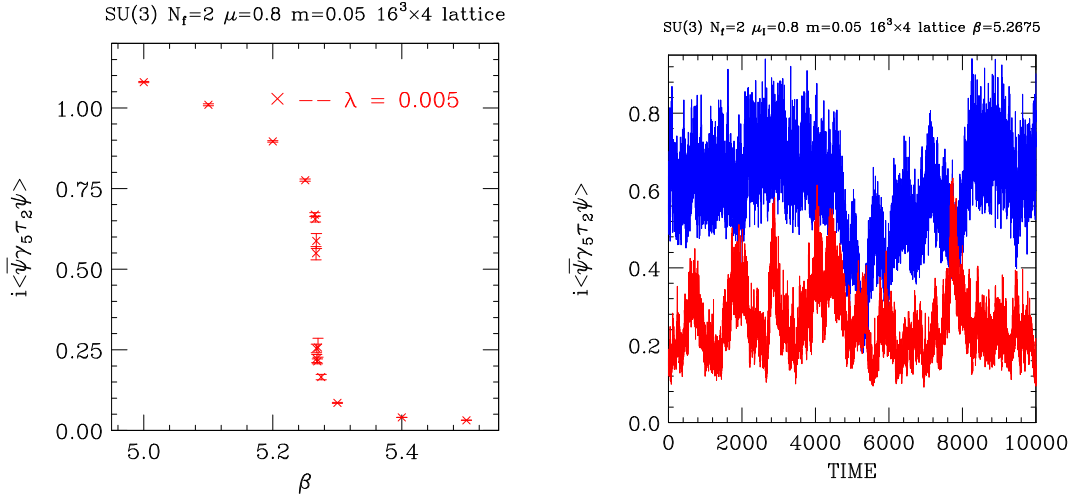


Fig. 8. a) Pion condensate as a function of $\beta = 6/g^2$ for $m = 0.05$ and $\mu_I = 0.8$. b) Pion condensates as functions of molecular-dynamics time at $\beta = 5.2675$ from hot and cold starts.

§4. The Spectrum of 2-colour QCD

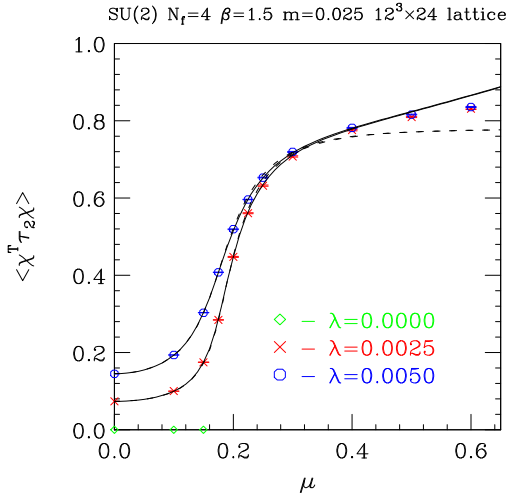
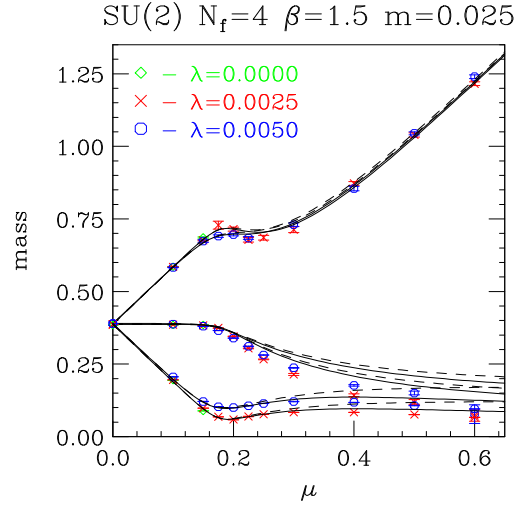
Lattice 2-colour QCD at finite chemical potential μ for quark number has the staggered fermion action

$$S_f = \sum_{sites} \left\{ \bar{\chi}[\mathcal{D}(\mu) + m]\chi + \frac{1}{2}\lambda[\chi^T\tau_2\chi + \bar{\chi}\tau_2\bar{\chi}^T] \right\} \quad (4.1)$$

This theory has a positive pfaffian which allows us to simulate it using the hybrid molecular-dynamics method. This lattice action has a $U(2)$ flavour symmetry when $m = \mu = \lambda = 0$. When this breaks spontaneously $U(2) \rightarrow U(1)$ giving rise to 3 Goldstone bosons. We have studied the behaviour of these bosons when these parameters are no longer zero. In particular we study the μ dependence when m is fixed at a value small enough to be within reach of chiral perturbation theory, and $\lambda \ll m$.^{2),7)}

At $\lambda = 0$ this theory has a phase transition at $\mu = m_\pi/2$ to a superfluid phase with a diquark condensate which spontaneously breaks quark-number. There is 1 true Goldstone boson. As for QCD at finite μ_I , the condensates and quark-number density are well described by a tree-level Lagrangian of the linear sigma model class. Figure 9 shows the diquark condensate, which is an order parameter for this transition as a function of μ and λ , as measured in simulations on a $12^3 \times 24$ lattice at $\beta = 4/g^2 = 1.5$ and $m = 0.025$.

We measure the μ and λ dependence of the 3 pseudo-Goldstone bosons and compare them with the predictions of the linear sigma model effective Lagrangian. (m_π is small enough at $m = 0.025$ for us to expect chiral perturbation theory to be valid.) Figure 10 shows the 3 (pseudo)-Goldstone boson masses as functions of μ . Although there is good qualitative agreement, quantitative agreement is lacking once μ is appreciably greater than $m_\pi/2$.


 Fig. 9. Diquark condensate as a function of μ .

 Fig. 10. Pseudo-Goldstone masses as functions of μ .

§5. χ QCD at finite μ and T .

We have formulated QCD with additional irrelevant chiral 4-fermion interactions which make the Dirac operator non-singular in the chiral limit (χ QCD).²⁶⁾ The staggered fermion part of this action is:

$$S_f = \sum_{\tilde{s}} \left\{ \bar{\chi} [\mathcal{D} + m + \frac{1}{16} \sum_i (\sigma_i + i\epsilon\pi_i)] \chi \right\} + \sum_{\tilde{s}} \frac{1}{8} N_f \gamma (\sigma^2 + \pi^2), \quad (5.1)$$

where \tilde{s} are the sites on the dual lattice, and the sum over i is the sum over the 16 sites on the dual lattice which are 1 unit away from the given site on the original lattice. It is just the properties which allow this action to be used in the chiral limit, that promise to make it better behaved than the standard staggered action at finite chemical potential.

Now consider what happens when we add a chemical potential μ in the usual way. Since the quark propagator on a single configuration no longer behaves as $\exp[-(m_\pi/2)|x - y|]$, but is controlled by $(\langle \sigma \rangle = \langle \bar{\chi} \chi \rangle / \gamma) + m$ rather than m , the phase of the determinant can remain well behaved for $\mu > m_\pi/2$, and even in the chiral limit.

Thus, provided we keep γ from becoming too large, the Swansea-Bielefeld expansion should be well behaved, even for $m = 0$. The hope is that the phase of the determinant will remain under control up to the critical end point. Since keeping γ “small” makes the flavour symmetry breaking bad, this should be considered as a model. It remains to see how well it represents QCD at finite μ .

In addition, we should be able to use this action to simulate with the magnitude of the determinant (equivalent to simulating at finite μ_I) at $m = 0$ and to search for the tricritical point. Here we see that the pion consisting of a quark from the

Dirac operator and an antiquark from the conjugate Dirac operator will be relatively heavy, which prevents it from causing problems at small μ .

Preliminary studies of this theory by Barbour, Kogut and Morrison²⁷⁾ suggest that χ QCD is indeed better behaved at finite μ than standard lattice QCD, and are consistent with the scenario presented above.

§6. Conclusions

QCD at finite isospin chemical potential and 2-colour QCD at finite quark-number chemical potential have some of the properties of QCD at finite quark/baryon-number chemical potential. Unlike QCD at finite μ , they have positive fermion determinants, so they are amenable to standard simulation methods.

QCD at finite μ_I has a phase transition with mean-field critical exponents to a superfluid phase in which isospin (I_3) and parity are broken by a charged pion condensate at $\mu_I = m_\pi$, as predicted by chiral perturbation theory. The dependence of the position of the finite temperature transition (T_c) on μ and on μ_I is the same for μ sufficiently small; so simulations at finite μ_I are a convenient way of estimating the μ dependence. We will check the agreement between our measurements and the Swansea-Bielefeld predictions. It appears that our results are consistent with those obtained by de Forcrand and Philipsen from simulations at imaginary μ .

Our 2-flavour simulations do not show any sign of the critical endpoint expected for QCD at finite μ and hence μ_I . Perhaps the tricritical point on the boundary of the pion condensed phase, where the transition changes from second order to first order, is a remnant of this endpoint. Unfortunately this is in the region where we cannot relate the finite μ_I and finite μ behaviour of lattice QCD.

For 2+1 flavours Fodor and Katz were able to determine the position of the critical endpoint at finite μ .^{18),19),20)} De Forcrand and Philipsen have made a determination of the position of this critical endpoint for 3 flavours by continuation from imaginary μ .²⁸⁾ (Similar determinations have been made for 4 flavours by D'Elia and Lombardo.²⁹⁾) The Bielefeld-Swansea collaboration have also determined the position of the critical endpoint for 3 flavours using their series expansions around $\mu = 0$.³⁰⁾ In addition to the fact that 2+1 flavours describes the real world, 2+1 or 3 flavours have the advantage that for small enough quark masses, the critical endpoint is at the origin. This means that one can arrange for the critical endpoint to be as close to $\mu = 0$ as one desires by tuning the quark masses, and follow its trajectory as these masses are increased. In particular, in a 3-flavour version of QCD at finite μ_I , we should be able to arrange for the critical endpoint to occur for $\mu_I < m_\pi$, where it should be related to the critical endpoint at finite μ . We are currently extending our QCD at finite μ_I simulations to 3 flavours, ignoring the fact that the theory we are simulating is not expected to have a sensible continuum limit, and hope to determine the position of this endpoint with good precision.

There remain some questions to be answered concerning QCD at finite μ_I . These include: Does pion condensation at finite isospin density occur when the system is also at finite baryon-number density? If so, how large can the baryon-number density become before pion condensation no longer occurs? How well does the pseudo-

Goldstone spectrum of lattice QCD at finite μ_I compare with the predictions of chiral perturbation theory?

The pseudo-Goldstone spectrum of 2-colour lattice QCD at finite μ shows semi-quantitative agreement with the predictions of effective chiral Lagrangians.

The χ QCD action shows promise for simulations at finite μ at T . It should allow determination of the critical endpoint for small (or even zero) quark masses.

Acknowledgments

DKS is supported by the US Department of Energy, Division of High Energy Physics, under Contract W-31-109-Eng-38. JBK and DT are supported in part by NSF grant NSF-PHY-0102409. DT is supported in part by “Holderbank”-Stiftung. These simulations were performed on the IBM SP at NERSC, the IBM SP at NPACI, the Jazz Linux cluster at LCRC, Argonne and on Linux PCs in the Argonne HEP Division.

References

- 1) S. Hands, J. B. Kogut, M. P. Lombardo and S. E. Morrison, Nucl. Phys. B **558** (1999) 327 [arXiv:hep-lat/9902034].
- 2) J. B. Kogut, D. K. Sinclair, S. J. Hands and S. E. Morrison, Phys. Rev. D **64** (2001) 094505 [arXiv:hep-lat/0105026].
- 3) J. B. Kogut, M. A. Stephanov and D. Toublan, Phys. Lett. B **464** (1999) 183 [arXiv:hep-ph/9906346].
- 4) J. B. Kogut, M. A. Stephanov, D. Toublan, J. J. Verbaarschot and A. Zhitnitsky, Nucl. Phys. B **582** (2000) 477 [arXiv:hep-ph/0001171].
- 5) K. Splittorff, D. Toublan and J. J. Verbaarschot, Nucl. Phys. B **620** (2002) 290 [arXiv:hep-ph/0108040].
- 6) J. B. Kogut, D. Toublan and D. K. Sinclair, Phys. Lett. B **514** (2001) 77 [arXiv:hep-lat/0104010].
- 7) J. B. Kogut, D. Toublan and D. K. Sinclair, Phys. Rev. D **68** (2003) 054507 [arXiv:hep-lat/0305003].
- 8) J. B. Kogut and D. K. Sinclair, Phys. Rev. D **66** (2002) 034505 [arXiv:hep-lat/0202028].
- 9) D. T. Son and M. A. Stephanov, Phys. Rev. Lett. **86** (2001) 592 [arXiv:hep-ph/0005225].
- 10) D. T. Son and M. A. Stephanov, Phys. Atom. Nucl. **64** (2001) 834 [Yad. Fiz. **64** (2001) 899] [arXiv:hep-ph/0011365].
- 11) E. V. Shuryak, Nucl. Phys. Proc. Suppl. **83** (2000) 103 [Phys. Atom. Nucl. **64** (2001) YAFIA,64,628-632.2001] 574 [arXiv:hep-ph/9908290].
- 12) M. G. Alford, Ann. Rev. Nucl. Part. Sci. **51** (2001) 131 [arXiv:hep-ph/0102047].
- 13) P. de Forcrand and O. Philipsen, Nucl. Phys. B **642** (2002) 290 [arXiv:hep-lat/0205016].
- 14) J. B. Kogut and D. K. Sinclair, Nucl. Phys. Proc. Suppl. **119** (2003) 556 [arXiv:hep-lat/0209054].
- 15) J. B. Kogut and D. K. Sinclair, arXiv:hep-lat/0309042.
- 16) C. R. Allton *et al.*, Phys. Rev. D **66** (2002) 074507 [arXiv:hep-lat/0204010].
- 17) C. R. Allton, S. Ejiri, S. J. Hands, O. Kaczmarek, F. Karsch, E. Laermann and C. Schmidt, Phys. Rev. D **68** (2003) 014507 [arXiv:hep-lat/0305007].
- 18) Z. Fodor and S. D. Katz, Phys. Lett. B **534** (2002) 87 [arXiv:hep-lat/0104001].
- 19) Z. Fodor and S. D. Katz, JHEP **0203** (2002) 014 [arXiv:hep-lat/0106002].
- 20) Z. Fodor, S. D. Katz and K. K. Szabo, Phys. Lett. B **568** (2003) 73 [arXiv:hep-lat/0208078].
- 21) Y. Hatta and K. Fukushima, arXiv:hep-ph/0307068.
- 22) K. Fukushima, Phys. Rev. C **67** (2003) 025203 [arXiv:hep-ph/0209270].
- 23) A. Mocsy, F. Sannino and K. Tuominen, Phys. Rev. Lett. **91** (2003) 092004 [arXiv:hep-ph/0301229].
- 24) A. Mocsy, F. Sannino and K. Tuominen, arXiv:hep-ph/0308135.

- 25) A. M. Ferrenberg and R. H. Swendsen, Phys. Rev. Lett. **61** (1988) 2635.
- 26) J. B. Kogut, J. F. Lagae and D. K. Sinclair, Phys. Rev. D **58** (1998) 034504 [arXiv:hep-lat/9801019].
- 27) I. M. Barbour, J. B. Kogut and S. E. Morrison, Nucl. Phys. Proc. Suppl. **53** (1997) 456 [arXiv:hep-lat/9608057].
- 28) P. de Forcrand and O. Philipsen, Nucl. Phys. B **673** (2003) 170 [arXiv:hep-lat/0307020].
- 29) M. D'Elia and M. P. Lombardo, Phys. Rev. D **67** (2003) 014505 [arXiv:hep-lat/0209146].
- 30) F. Karsch, C. R. Allton, S. Ejiri, S. J. Hands, O. Kaczmarek, E. Laermann and C. Schmidt, arXiv:hep-lat/0309116.